

Szymon Sobura¹, Beata Hejmanowska², Małgorzata Widłak³, Joanna Muszyńska⁴

The Application of Remote Sensing Techniques and Spectral Analyzes to Assess the Content of Heavy Metals in Soil – A Case Study of Barania Góra Reserve, Poland

Abstract: The understanding of the spatial and temporal dynamics of farmland processes is essential to ensure the proper crop monitoring and early decision making needed to support efficient resource management in agriculture. By creating appropriate crop management strategies, one can increase harvest efficiency while reducing costs, waste, chemical spraying, and inhibiting the impact of biotic and abiotic factors on crop stress. Only reliable spatial information makes it possible to comprehend the influence of various factors on the environment. The main objective of the research presented in the paper was to assess the possibility of using maps of vegetation and soil indices, such as NDVI, SAVI, IRECI, $CI_{red-edge}$, PSRI and HMSSI, calculated on the basis of images from the Sentinel-2 satellite, to qualitatively determine the increased amount of heavy metals in the soil in the areas of small agricultural plots around the Barania Góra nature reserve in Poland. The conducted pilot project shows that the spectral indices: NDVI, SAVI, IRECI, $CI_{red-edge}$, PSRI, and HMSSI, calculated on the basis of images from Sentinel-2, have the potential to assess the content of nickel, zinc, chromium and cobalt in the soil on agricultural plots. However, the confirmation of the obtained results requires continuation of the research.

Keywords: remote sensing, heavy metals, Sentinel-2, soil, spectral indices

Received: 13 May 2022; accepted: 13 September 2022

© 2022 Authors. This is an open access publication, which can be used, distributed and reproduced in any medium according to the Creative Commons CC-BY 4.0 License.

¹ Kielce University of Technology, Faculty of Environmental, Geomatic and Energy Engineering, Kielce, Poland, email: ssobura@tu.kielce.pl,  <https://orcid.org/0000-0002-8678-6264>

² AGH University of Science and Technology, Faculty of Geo-Data Science, Geodesy, and Environmental Engineering, Krakow, Poland, email: galia@agh.edu.pl,  <https://orcid.org/0000-0003-0230-8386>

³ Kielce University of Technology, Faculty of Environmental, Geomatic and Energy Engineering, Kielce, Poland, email: mwidlak@tu.kielce.pl,  <https://orcid.org/0000-0001-6195-4746>

⁴ Kielce University of Technology, Faculty of Environmental, Geomatic and Energy Engineering, Kielce, Poland, email: jdlugosz@tu.kielce.pl,  <https://orcid.org/0000-0001-7486-4141>

1. Introduction

The soil is one of the key components of ecosystems and vital to ensure the proper existence of humans and animals. As an area of agricultural production, the soil is constantly exposed to human activity, which translates into soil degradation, pollution with heavy metals, erosion, and salinity. Soil is a basic and non-renewable element of the natural environment [1]. Many scientific papers have emphasized the importance of soil protection against degradation, both within individual countries and throughout the EU [1–3]. Heavy metals and petroleum hydrocarbons are the most common soil contaminants. Heavy metals that enter the biosphere are not subject to degradation processes, which is particularly dangerous due to the successive accumulation of their content over time, their toxicity, and their easy assimilation by plants. The harmfulness of excessive heavy metals content is a common feature in the context of their impact on the environment and humans, therefore it is important to study the presence of heavy metals in various biological systems [4]. A high content of lead (Pb) in the soil negatively affects the growth and quantity of crops. In turn, cadmium (Cd), as one of the most phytotoxic heavy metals absorbed by vegetables due to its fat solubility, may pose a serious threat to human health [5, 6]. Copper (Cu) and zinc (Zn) in low concentrations are essential micronutrients for plants, but their increased content in the soil can be toxic and delays vegetation, and even causes the death of most plant species [7]. Only accurate and timely mapping of agricultural land can ensure food and economic security [8].

As a result, the uncontrolled accumulation of heavy metals in the soil on agricultural land may lead to environmental contamination or the absorption of heavy metals by crops, and thus enter the trophic chain. Moreover, heavy metals can destroy the normal functioning of the soil and cause stress in crops, and additionally hinder their vegetation [5, 6]. It should be emphasized that the content of heavy metals in soils is regulated by separate standards and only the exceeding of recommended standards adversely affects human health. Because of the rapid physical development of young people, their absorption index is higher, which may exacerbate the problem of heavy metal accumulation in children, and the effects may appear after prolonged exposure to this phenomenon [1]. Many researchers have focused their scientific interests on the quantification of heavy metals content with the use of various modern techniques and tools in the form of multispectral images and machine learning [5, 9–11], which additionally emphasized the importance of this issue. In China alone, contaminated land accounts for one-sixth of all cultivated soil. Only an understanding of the phenomena causing such a situation allows the implementation of remedial measures to improve the quality of agriculture [6].

The main aim of the research presented in the paper was to assess the possibility of using maps of vegetation and soil indices, such as NDVI (Normalized Difference Vegetation Index), SAVI (Soil Adjusted Vegetation Index), IRECI (Inverted Red-Edge Chlorophyll Index), $CI_{\text{red-edge}}$ (Chlorophyll Index red-edge), PSRI (Plant

Senescence Reflectance Index), and HMSSI (Heavy Metal Stress Sensitive Index), calculated from images taken by the Sentinel-2 satellite, to qualitatively determine the increased amount of heavy metals in the soil in the areas of small agricultural plots around the Barania Góra reserve. An indirect task to be performed in order to achieve the goal consisted in analyzing the content of heavy metals in the agricultural areas around the Barania Góra reserve, which is in the vicinity of the Natura 2000 area with code PLH260010.

2. Literature Review

D'Emilio et al. [1] discusses the research on the concentration of heavy metals in the soil and the commonly used NDVI spectral index in southern Italy, an area strongly affected by the anthropogenic activity of the oil extraction industry. The obtained results indicate the existence of a relationship between the anomalies of plant activity and the physicochemical characteristics of the soil. This means that a satellite remote sensing technician can find applications for monitoring an area subject to a negative external influence. This approach allows to minimize the workload and costs associated with traditional field works [1]. Similar conclusions have been reached by many researchers [5, 11], who undertook the use of hyperspectral imaging to monitor the soil contamination with heavy metals in agricultural areas, in order to identify crops potentially threatened with hazardous chemical components. On the other hand, Liu et al. [10] investigated the issue of the prediction of soil contamination with heavy metals (Cd, Hg, Pb), using narrow bands of the electromagnetic radiation spectrum in various ranges and statistical methods, including multivariate regression, obtaining satisfactory results which are in agreement with the results of other scientists. The study of the relationship between the plant phenology and the stress, caused by the abiotic factor in the form of heavy metals, additionally allows to interpret correctly the response of the plant species under study to the concentration of heavy metals in the soil [6]. The reflectivity for electromagnetic waves with a wavelength of 450, 550, and 670 nm gives satisfactory results for monitoring the concentration of selected heavy metals in plants. A statistically significant correlation between the value of the spectral reflection in the red-edge channel and the concentration of heavy metals has been confirmed by a number of studies [12, 13].

Over the last decade or so there has been an increased interest in precision farming, both at the level of the agricultural community and food consumers. The European Union aims to reform the Common Agricultural Policy (CAP) in the coming years. The Integrated Management and Control System (IACS) implements development payments for farmers in terms of area, using satellite images of high and very high resolution. The abundance of free data available under the European Copernicus program encourages Member States to implement the IACS, using Sentinel images to monitor agricultural parcels [14, 15]. For example, the determination of the type

and spatial distribution of crops is key to forecasting national yields. This is important in the context of determining the amount of food that can be stored in warehouses and exported abroad [8]. By creating appropriate crop management strategies, it is possible to increase the harvest efficiency while reducing costs, waste, chemical spraying and inhibiting the influence of biotic and abiotic factors on the stress of cultivated plants [16, 17]. Heavy metals, apart from being a threat to the environment, lower the productivity of plants. The use of phytoremediation technology is one of the reclamation techniques for areas affected by contamination with heavy metals or the action inhibiting the accumulation of such elements in the soil [7]. However, this technology is not always cost effective. Because of the rising demand for food and the growing world population, it is necessary to conduct research in order to maximize production and minimize the impact of negative external factors on the quantity and quality of crops [17]. Growing cereals requires sustainability not only in terms of production but also its environmental impact. The very availability of nitrogen in soil varies spatially within the cultivated plants and depends on the physicochemical properties of the soil, including its morphology [18].

The potential of remote sensing for plant health monitoring and crop mapping has been highlighted in many studies [19–22]. Global warming and the related climate forecasts indicate an increased probability of droughts, which will put additional pressure on the water sector and contribute to the build-up of problems in agriculture and an increased level of stress on plants. The abiotic groups of stress factors, which negatively affect the quality of the soil and the size of crops, apart from water deficiency, extreme temperatures, and nutrient deficiency, also include an increased content of heavy metals [23]. This may include increased crop stress in the monitored areas. Therefore, it is extremely important to monitor the condition of crops and develop strategies that will help ensure the safety of both food and water [24]. Agricultural decisions can impact the local community in many ways, including increased fertilization and exposure to pesticides, one of the sources of increased levels of heavy metals in the soil. The use of remote sensing techniques to create and update maps of crop and plant growth is the next step in the development of precision farming.

Phenological information obtained by means of remote sensing sensors allows the study of the growth and state of stress in plants practically all year round. This limits the uncertainty of the selection of the spectral response, sensitive to changes in the physical parameters of the environment [6]. By the use of remote sensing techniques, it is possible to take into account biotic and abiotic stress factors, and thus update the Liebig's minimum law, assuming that growth factors such as water and temperature are optimal, to the current climate situation and technological progress in the world [23]. The performance of soil monitoring tasks for large areas and in repetitive periods of time is problematic for people involved in soil testing. With the use of correlation analyzes between the calculated reflectance value and the content of heavy metals in the soil, it is possible to remotely monitor the soil quality [10, 25].

The presence of heavy metals in the soil influences the speed of microbiological processes, including decomposition, which is necessary to ensure soil fertility and long-term plant productivity. In the study reported by Zhang et al. [26], the spectral index IRECI (Inverted Red-Edge Chlorophyll Index) was already examined in terms of monitoring the changes in the concentration of heavy metals in large areas subjected to reclamation after an inactive ore mine, giving results that were satisfactory for the authors. On the other hand, radar data from Sentinel-1 since 2015 can provide useful information for the agricultural sector. Polarized VH / VV radar images are consistent with the value of the GAI (Green Area Index) spectral index and the biomass of the crop [14]. This means that radar imaging allows for an additional enrichment of the observation resource for a thorough assessment of the soil quality and its relationship with other physicochemical parameters in the analyzed area [27, 28].

An accurate determination of the content of heavy metals in the soil is possible due to in situ measurements and analytical methods. These methods have limitations as they are both time- and cost-consuming. Another problem is a spot nature of the measurement, usually with a limited spatial density, which in the case of high spatial variability of physicochemical parameters makes it practically impossible to perform a reliable interpolation. Thus, efforts are being made to create new, indirect techniques for determining the values describing the state of the environment, using remote methods, e.g., satellite remote sensing and image spectroscopy. The approach of remote sensing, which allows for repeated contactless coverage of relatively large areas with images, has become attractive for the purposes of identifying and assessing spatial patterns of physical and biochemical properties of soils [10]. These techniques offer the ability to conduct research over a large area, but are sensitive to weather conditions (the presence of cloud cover, excessive humidity), which brings about the need for advanced radiometric corrections of such scenes. In the literature review, one can find many applications of remote sensing for the analysis of drought phenomena, soil moisture mapping, interpretation of the viability and productivity of crops or analyzes of vegetation and soil itself [20, 24, 25, 27]. Many satellite programs, such as Landsat, SPOT, Sentinel-1, and Sentinel-2, provide collections of their images for free. One of the limiting factors in the use of satellite images are gaps in the acquired time series, resulting from the low frequency of revisits and high cloudiness. The spatial integration of data from several satellites is therefore of particular importance for optical sensors, allowing for multi-time analyzes and may be a solution to the above-mentioned problem [16, 19].

3. Study Area

The subject of the assessment consisted of the agricultural land located on four test sites around the Barania Góra (Sheep Mountain) reserve in the Świętokrzyskie voivodship, Poland, situated approximately 16 km north-west of the city of Kielce.

The Barania Góra nature reserve was established in 1993 and covers an area of 82 ha. It was established to preserve diverse forest communities, including loess ravines, and to protect common ivy. The total area of all test sites used in the experiment was 3.6 ha. The area around the testing grounds is classified as Natura 2000 habitat areas. Currently, there is no impact factor in the form of industrial plants around the analyzed areas. The presented areas are used for the cultivation of grain. The exact arrangement of the samples is presented in Figure 1 (description of the attached location coordinates in EPSG: 2180).

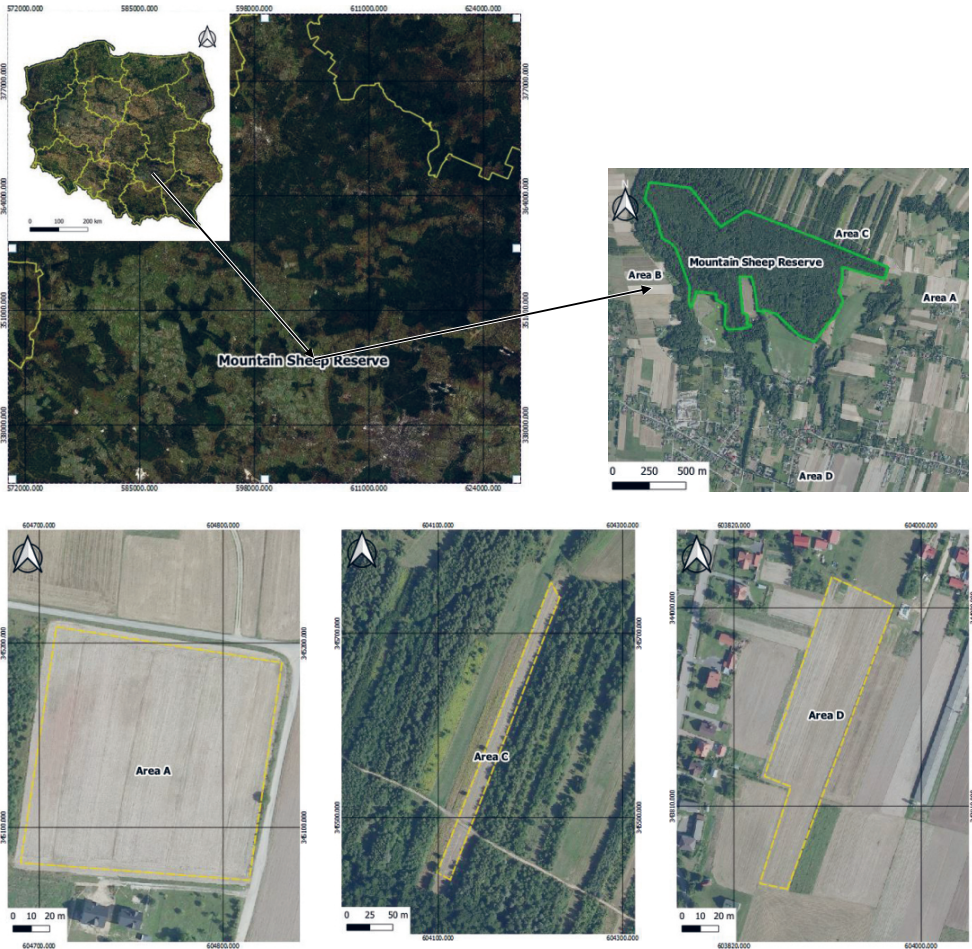


Fig. 1. Location of the test sites around the Barania Góra reserve, Poland

The A (1.6 ha) and C (0.5 ha) test sites are located far from buildings. The test site D (1.5 ha) is located in the vicinity of dense development of single-family houses and poultry farming. The height differentiation of the experimental test sites reaches

almost 110 m in relation to the highest and lowest study area. The average horizontal distances between the sampling points range between 700 and 1,600 m. The range of the experimental test sites was selected in such a way that the analyzed areas differed not only in terms of their area, but also in the contour shape and in their surroundings.

There were two main reasons why the authors chose the presented area for research. The presented agricultural areas are used for the production of grain as a feed ingredient for local farms. The second reason was the assessment of the state of the environment in terms of heavy metals content in the close vicinity of the protected Barania Góra nature reserve, which is within the range of the Natura 2000 area, code PLH260010 – Suchedniowskie Forests. Over 12 protected species listed in the Council Directive 92/43 EEC were found in the area. Combining the above, the authors concluded that conducting a pilot research project here would benefit the local area. Because of the high activity of agricultural machinery and the use of pesticides in the area, researchers assumed that there was a risk of heavy metals accumulation in the soil that should be controlled.

4. Research Methodology

4.1. Methodological Overview

Analyzes based on the study of bands of electromagnetic radiation highly correlated with the chemical properties of soil are, according to [10], the most fundamental analyzes.

Figure 2 presents an overview diagram presenting the research used. The whole methodology can be divided into three main parts, i.e., chemical analysis (Section 4.2), analyzes related to the use of multispectral imagery (Section 4.3), and statistical analyzes (Section 4.4).

From the saved position, vector files were created in the GIS software which comprised the scope of each area. Satellite images recorded by the MSI sensor, were downloaded and pre-processed in the software recommended by the ESA, SNAP. There was a difference of 4 days between the date when the soil samples were taken and the time Sentinel-2 images were taken. No unstable meteorological conditions in the form of snowfall or rainfall were observed during this period, and the difference in daily temperatures recorded in this period did not exceed 3°C. Therefore, it was found that ground-based measurements were representative for further analyzes in relation to satellite data, which is consistent with the experience of other researchers [29, 30].

Using the previously prepared vector masks, two fragments corresponding to the range of three experimental test sites A, C, and D were cut from the Sentinel satellite images, which were subjected to detailed tests described in section 4.3. Testing

ground B was not subjected to additional analyzes due to the fact that this area was covered with clouds when the pictures were taken by the satellite, which had a negative impact on the recorded value of the electromagnetic radiation reflection.

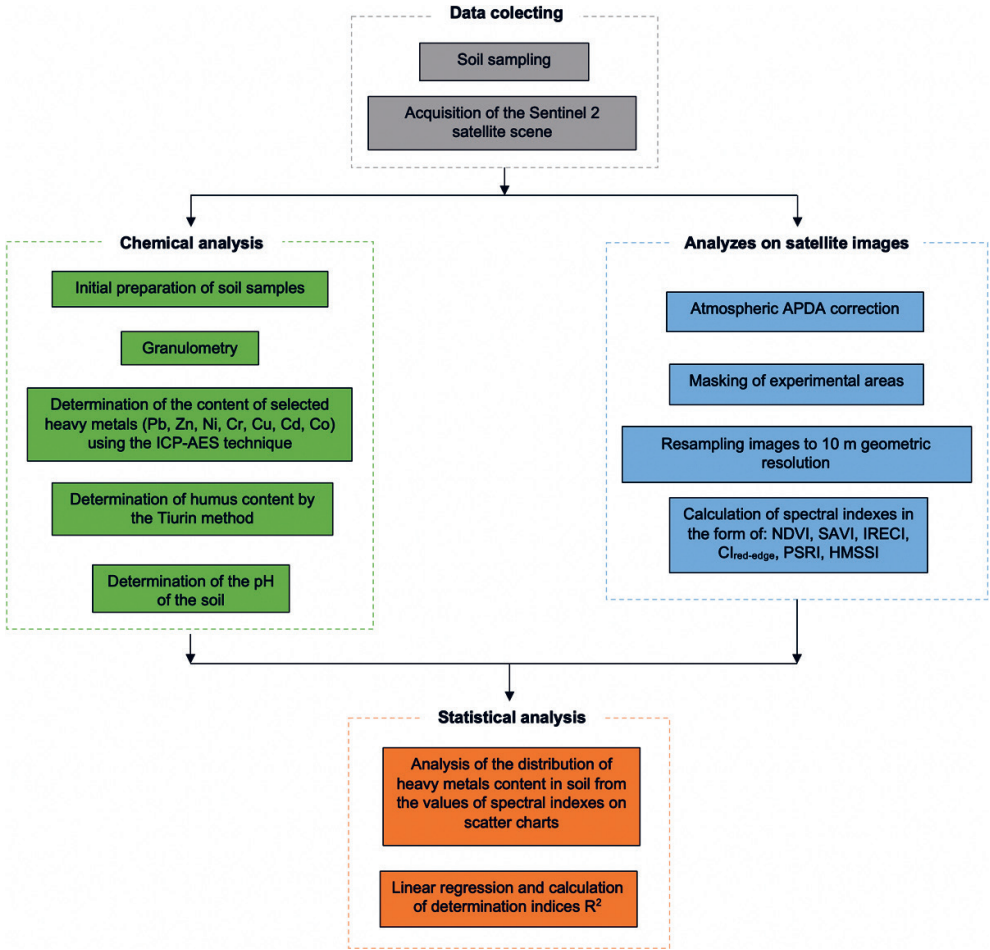


Fig. 2. The methodology of the conducted research

4.2. Chemical Analyzes

Samples for laboratory chemical analyzis were taken from the soil with an Egner’s cane from a depth of 40 cm [31]. The volume of a single soil sample was about 1.5 dm³. The sampling site coordinates were recorded using the autonomous GNSS position available in a mobile device with a situational accuracy of ±2.5 m. Mixed and air-dry samples were analyzed. There were 30 to 40 samples taken in the test cycle from each test site. The field samples were collected at similar spaces, creating

a Z-shape. The particle size distribution was determined by laser diffraction in accordance with the ISO 14887:2000, using a Mastersizer 3000 [32, 33]. The total contents of metals: Cd, Cu, Co, Cr, Ni, Pb, and Zn was determined using the ICP-AES technique after mineralization of the samples with aqua regia in accordance with the EN 13346:2000 standard [34]. The measurement accuracy by the ICP-AES technique was 0.001 mg/kg. The soil pH in 1MKCl was potentiometrically determined using a Mettler Toledo pH meter [35]. The humus was calculated from the organic carbon content determined by the Tiurin method [36].

The results of the chemical analyzes were used to validate the spectral indices calculated on the basis of multispectral images from Sentinel-2.

4.3. Analyzes of Data from Sentinel-2 Images

The information obtained in situ may be unrepresentative for the entire area, especially during large-scale studies over a large area [10]. Satellite images allow us to analyze even large areas in short time intervals. For the purposes of the experiment, the images taken on December 21, 2019, recorded by the Sentinel-2 satellite, were used. Images downloaded from the EarthExplorer website [<https://earthexplorer.usgs.gov/>] were radiometrically corrected in the SNAP software dedicated to the processing of satellite images. The satellite is equipped with an MSI push-broom scanner, recording 13 spectral channels with different geometric and spectral resolution. Table 1 presents the detailed characteristics of the Sentinel-2 channels used [37].

Table 1. Specification of the spectral channels of the Sentinel-2 satellite

Band number	Central wavelength [nm]	Bandwidth [nm]	Spatial resolution [m]
1: Coastal Aerosol	443.9	27	60
2: Blue	496.6	98	10
3: Green	560.0	45	10
4: Red	664.5	38	10
5: Red-edge 1	703.9	19	20
6: Red-edge 2	740.2	18	20
7: Red-edge 3	782.5	28	20
8: NIR	835.1	145	10
8a: NIR Narrow	864.8	33	20
9: Water Vapor	945.0	26	60
10: SWIR Cirrus	1,373.5	75	60
11: SWIR	1,613.7	143	20

Source: <https://sentinels.copernicus.eu/web/sentinel/home>

The downloaded satellite images were at the L1C processing level. Atmospheric correction was performed according to the APDA (Atmospheric Precorrected Differential Absorption) algorithm and the Sen2Cor function, based on the determination of the water vapor content from the L1C level images [38]. After radiometric correction, the images were brought to the level of L2A processing, which were further used in the research. Spectral channels with a geometric resolution of 60–20 m were resampled to a size of 10 m.

Various spectral indices calculated on the basis of the recorded spectral response by the satellite were used in the research. The indices employed can be divided into two groups: concerning plant vegetation and soil condition. The work focused on the following spectral indices: NDVI, SAVI, IRECI, $CI_{\text{red-edge}}$, PSRI, and HMSSI.

The NDVI index is one of the most recognizable and widely used spectral indices in agriculture [39]. It is strongly correlated with the concentration of chlorophyll concentrated in the plant assimilation apparatus and is expressed by equation (1):

$$NDVI = \frac{\rho_{NIR} - \rho_{RED}}{\rho_{NIR} + \rho_{RED}} \quad (1)$$

where ρ_{NIR} are the DN (Digital Number) values, which are a measure of electromagnetic radiation reflection in the near infrared range, and ρ_{RED} are the red reflection values of the optical radiation band. The values of the NDVI index range from -1 to 1, where low values indicate no or poor course of vegetation, and high values of the index – increased vegetation.

The spectral SAVI (Soil Adjusted Vegetation Index), calculated with formula (2), is a modification of the NDVI index. It allows the influence of soil brightness to be taken into account in relation to the surroundings [40]. It is used to assess the condition of plants at an early stage of vegetation, when the assimilation apparatus is not sufficiently developed:

$$SAVI = \frac{\rho_{NIR} - \rho_{RED}}{\rho_{NIR} + \rho_{RED} + L} \cdot (1 + L) \quad (2)$$

where L is the area covered with vegetation. In the discussed research, the value of $L = 0.5$ was used.

The IRECI (Inverted Red-Edge Chlorophyll Index) is calculated on the basis of the value of the spectral response from four bands of recorded satellite channels, according to formula (3). The use of red and three infrared spectral channels allows to estimate the chlorophyll content in plants. The reflection of the red edge in formula (3) is used as an indicator of stress and aging of the vegetation [37].

$$\text{IRECI} = \frac{\rho_{\text{NIR}} - \rho_{\text{RED}}}{\rho_{\text{RED-EDGE 1}} / \rho_{\text{RED-EDGE 2}}} \quad (3)$$

where $\rho_{\text{RED-EDGE 1}}$ and $\rho_{\text{RED-EDGE 2}}$ are the respective spectral channels of Sentinel-2 from Table 1.

Another index related to the content of chlorophyll in plants is the $\text{CI}_{\text{red-edge}}$ spectral index (Chlorophyll Index red-edge), calculated based on formula (4). The advantage of its use consists in a linear dependence of the index value on the content of chlorophyll. Low values of the $\text{CI}_{\text{red-edge}}$ index may indicate a low content of chlorophyll and high plant stress [41]:

$$\text{CI}_{\text{red-edge}} = \frac{\rho_{\text{RED-EDGE 3}}}{\rho_{\text{RED-EDGE 1}}} - 1 \quad (4)$$

The PSRI index (Plant Senescence Reflectance Index) – unlike the previously presented index – is more sensitive to the ratio of carotenoids to chlorophyll. For Sentinel-2 images it is calculated as in formula (5). An increased PSRI value indicates an increased stress in plants [26]. PSRI values range from -1 to 1.

$$\text{PSRI} = \frac{\rho_{\text{RED}} - \rho_{\text{BLUE}}}{\rho_{\text{RED-EDGE 2}}} \quad (5)$$

The last spectral index tested was the Heavy Metal Stress Sensitive Index (HMSSI), proposed by [41], and calculated according to formula (6). It combines the advantages of the two previous indices. If the plants exhibit stress, the $\text{CI}_{\text{red-edge}}$ value decreases, while in the same situation the PSRI value increases. As a result, the HMSSI indicator is more sensitive to plant stress, which may be reflected in the detection of an increased concentration of heavy metals.

$$\text{HMSSI} = \frac{\text{CI}_{\text{red-edge}}}{\text{PSRI}} \quad (6)$$

4.4. Statistical Analyzes

The R^2 coefficient of determination was adopted as a measure of the relationship between the obtained observations. Liu et al. [10] and Choe et al. [11] have shown that it is possible to create a simple mathematical model allowing to link the radiation spectrum (in certain ranges of electromagnetic radiation) with the content of heavy metals in soil. However, the possibility of creating a mathematical model to monitor the pollution with heavy metals for relatively small agricultural plots, that are not subjected to strong pressure from industrial plants, was not tested. The Pearson correlation

coefficient for the collected data was calculated using formula (7). The linear regression model was calculated using the least squares method for the most highly correlated spectral indices with the in situ measurements obtained in the research. By squaring the correlation coefficient r_{xy} the coefficient of determination R^2 was obtained:

$$r_{xy} = \frac{\sum_{i=1}^n (x_i - \bar{x})(y_i - \bar{y})}{\sqrt{\sum_{i=1}^n (x_i - \bar{x})^2} \sqrt{\sum_{i=1}^n (y_i - \bar{y})^2}} \tag{7}$$

In the presented studies x_i and y are the values of the calculated spectral indices and the content of heavy metals in the soil, and \bar{x} and \bar{y} are average values from the samples calculated for the entire range of the testing ground.

5. Results

5.1. Results of Chemical Analyzes

The results of the content of selected heavy metals in the tested samples are shown in Table 2 along with the errors in their determination. The last column of Table 2 shows the permissible value of heavy metal concentration in agricultural soil in Poland [42]. The presented value of the metal concentration is the sum of the metal content in all soil fractions. On the other hand, the standard deviation shown in Table 2 is related to soil samples from a given test site, which were then averaged, and from which the value of the heavy metals analyzed in the study was determined.

Table 2. Results of the concentration of heavy metals from the mixed test for the analyzed experimental test sites A, C, and D together with their permissible content in the soil for agricultural areas in Poland

Heavy metal	Area A (East)		Area C (North)		Area D (South)		Permissible contents of selected metals in soil
	Metal conc. in soil [mg/kg]	Std. dev.	Metal conc. in soil [mg/kg]	Std. dev.	Metal conc. in soil [mg/kg]	Std. dev.	Metal conc. in soil [mg/kg]
Cu	10.50	0.04	9.54	0.02	8.68	0.01	200.00
Cr	8.07	0.76	11.65	0.68	7.88	0.36	200.00
Ni	4.40	0.04	6.09	0.03	4.77	0.02	150.00
Pb	54.77	0.18	22.91	0.12	17.72	0.13	200.00
Zn	68.79	0.33	96.94	0.30	58.41	0.36	500.00
Co	2.43	0.05	4.82	0.04	2.77	0.02	50.00
Cd	1.73	0.01	1.31	0.02	0.89	0.01	2.00

In order to present the differences in the concentrations of heavy metals for the three analyzed experimental test sites, bar graphs were created as in Figures 3 and 4. Out of the seven analyzed heavy metals, an anomaly was observed in the form of an increased cadmium content on the eastern test site (marked with the letter A), i.e., 87% of the permissible value of the element content in agricultural soils. Phosphorus fertilizers are the source of cadmium in agricultural area, which constitute approximately 54%, approximately 5% is sewage used for soil fertilization, and approximately 41% is usually airborne [43]. The remaining contents of the tested metals in all test sites range from 3% to 13% of the standard. The content of heavy metals for the analyzed test sites is similar, except for lead, which is shown in Figures 3 and 4. However, the total contents of the tested metals do not exceed the applicable standard for agricultural land, presented in Table 2. Figure 4 shows the reference to the standard for cadmium content in agricultural areas in force in Poland.

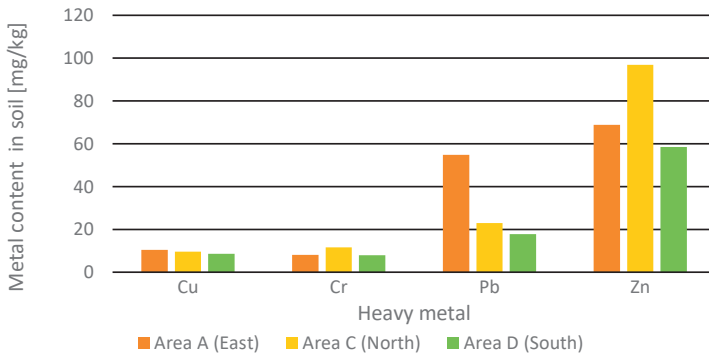


Fig. 3. The content of heavy metals Cu, Cr, Pb, and Zn in the soil for the analyzed experimental sites

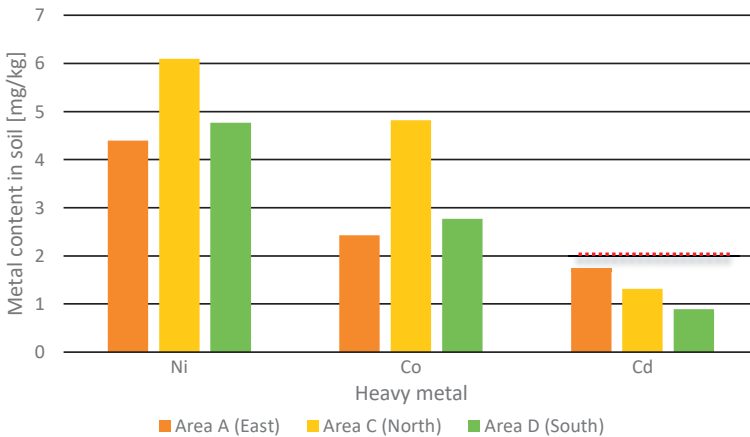


Fig. 4. Content of heavy metals Ni, Co, and Cd in the soil for the analyzed experimental sites with reference to the allowable cadmium content in Poland (red line)

The humus content and the pH level in the soils were checked in the three analyzed areas, A, C, and D soils rich in humus are more resistant to the influence of pollutants than low-humus soils [44]. Humus has a large water capacity and is characterized by a very large sorption capacity. Humus compounds increase the buffer capacity and regulate the pH of the soil solution [45]. The humus content in soils in Poland varies: for poor soils it is 0.1–1%, for poor humus soils – 1.01–2%, for medium humus soils – 2.01–4%, for humus soils – over 4% [44]. In the discussed study, each of the soils for the three test sites can be classified as a medium humus soil. Detailed parameters concerning the mean content of humus and the mean pH value for the analyzed test sites are presented in Table 3. The pH values for all the collected samples were in a range of pH 6.6–7.6, meaning there was no acidic environment in any of the test sites.

Table 3. Parameters of pH and humus on the measuring test sites around the Barania Góra reserve, Poland

Parameters	Sampling location		
	Area A (East)	Area C (North)	Area D (South)
Average pH value	6.6	7.0	7.6
Average humus content [%]	3.5	2.7	2.5

5.2. Results of Analyzes Based on Satellite Images

Figure 5 shows the outline of the experimental test sites against a background of satellite images. For images on the left only the detector was calibrated, which gave the top of atmosphere (TOA) reflectance. A color RGB composition shows a characteristic influence of the water vapor. The images on the right are after a full radiometric correction and the reflectance has been converted to the bottom of atmosphere (BOA). This is initially visible in the improved color of the presented color compositions.

The homogeneity of the samples in terms of the registered spectral response was tested. Area C turned out to be the test site with the lowest variability of the reflectance. Figure 6 presents graphs with spectral curves, after the initial (TOA) and full (BOA) radiometric correction for the three analyzed experimental areas. When comparing the spectral curves of corresponding test sites in Figure 6a and 6b it is possible to notice a significant improvement in radiometry after a full atmospheric correction of the images in the visible (VIS) and near infrared (NIR) bands. This means that the use of atmospheric correction is important in terms of spatial analyzes, which is confirmed by the results of studies by other authors [46].

Representative and commonly used spectral indices were determined: NDVI, SAVI, IRECI, $CI_{red-edge}$, PSRI, and HMSSI. The values of the obtained indices were to check the relationship between the selected indices and the content of heavy metals analyzed in this study. Figure 7 presents the distribution maps of spectral indices. Figures 7a and 7b show a different level of vegetation in the selected experimental sites, even though each of these areas was not covered with vegetation at the time of soil sampling. The high values of the NDVI and SAVI indices in areas A and D can be explained by early agricultural operations in the form of plowing and high ambient temperatures for the winter season, favoring plant vegetation and photosynthesis. The level of chlorophyll and the $CI_{red-edge}$ index in the studied areas is similar as shown in Figure 7d. The northern test site (area C) is less exposed to biotic and abiotic factors, which cause stress to vegetation, as indicated by lower PSRI values (Fig. 7e). The HMSSI index calculated on the basis of the red-edge CI and PSRI indices did not give satisfactory results, showing a large amount of "salt and pepper" noise, without a specific outline of the anomaly area.



Fig. 5. Testing grounds around the Barania Góra reserve, Poland

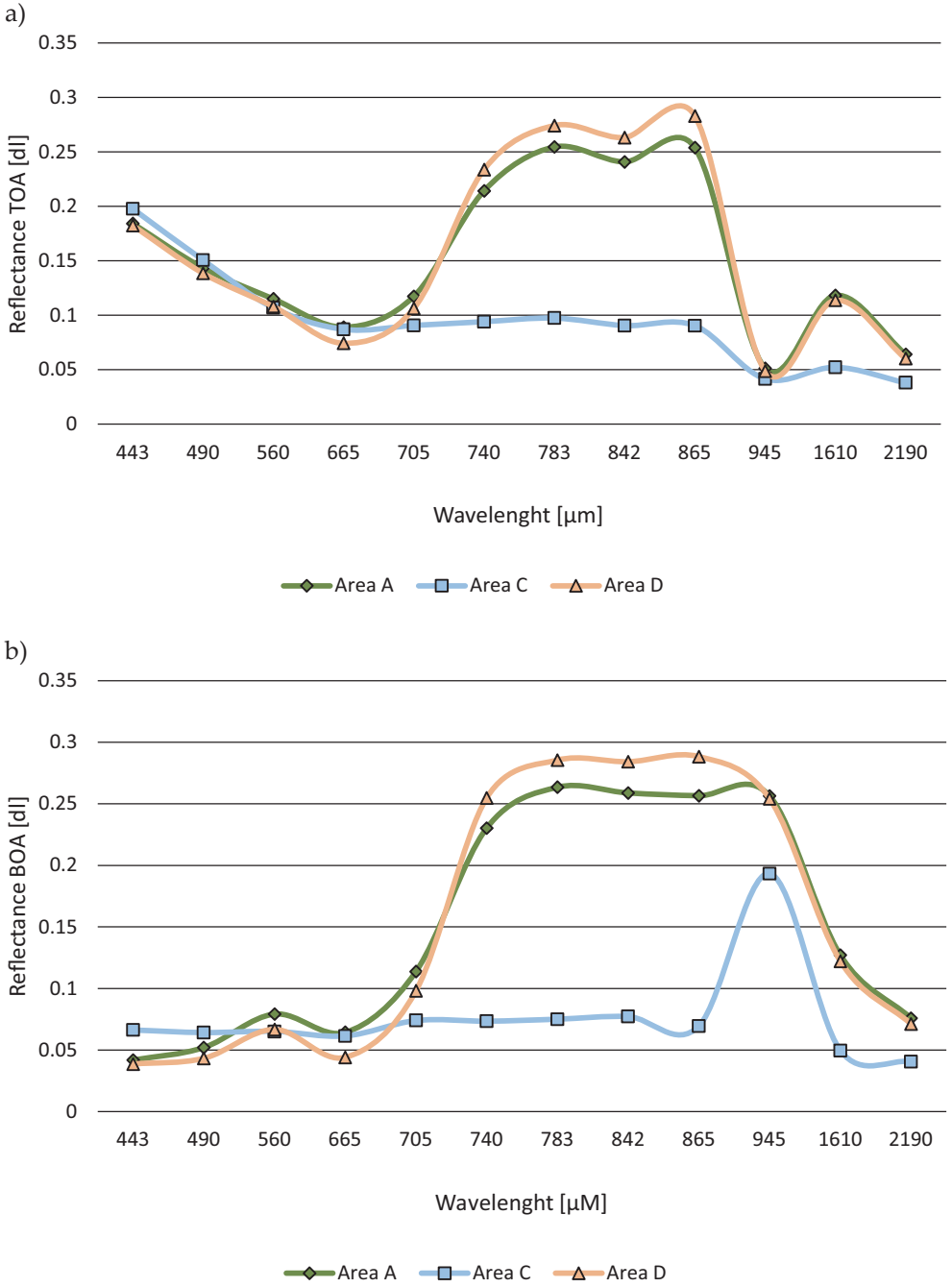


Fig. 6. Spectral curves for the analyzed experimental test sites A, C, and D:
a) before atmospheric correction (TOA);
b) after atmospheric correction (BOA)

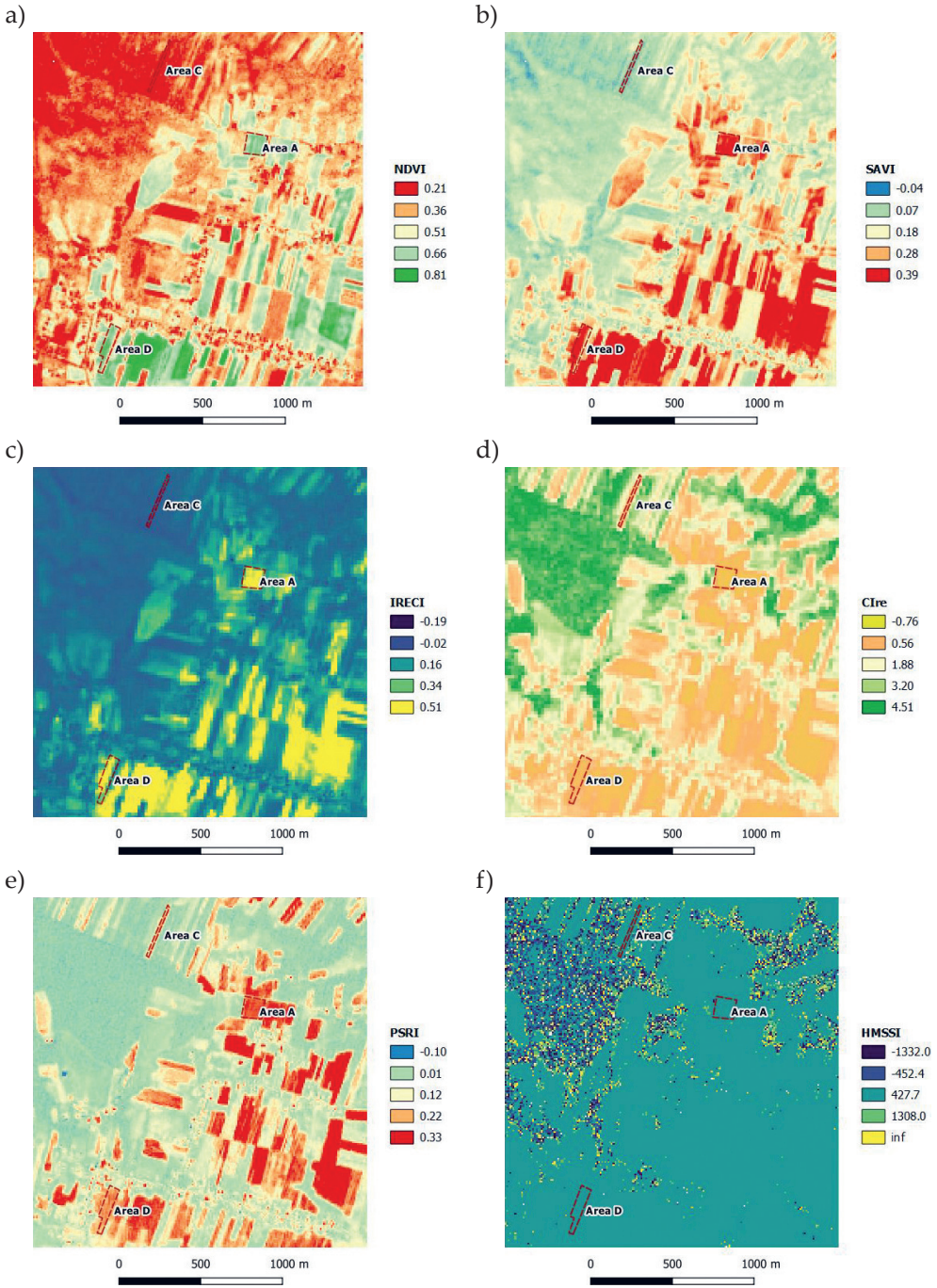


Fig. 7. Maps of spatial spectral indices around the tested experimental sites: a) NDVI index; b) SAVI index; c) IRECI index; d) $CI_{red-edge}$ index; e) PSRI index; f) HMSST index

5.3. Results of Qualitative Analyzes

The obtained values of the six spectral indices (Fig. 7) for the specified test sites A, C, and D, were averaged and visualized in Figures 8a and 8b.

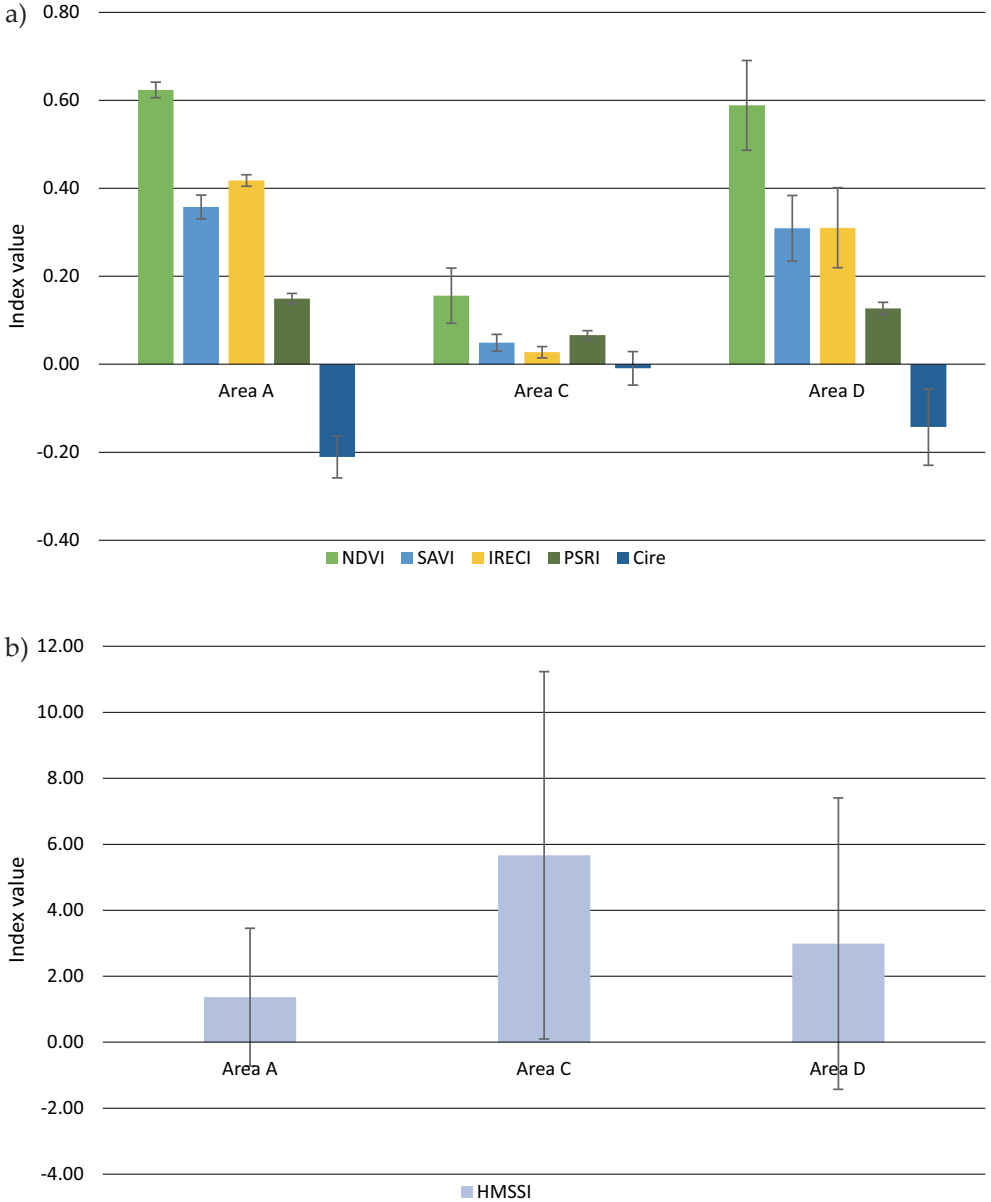


Fig. 8. Summary of averaged values of spectral indices for A, C, D experimental sites: a) NDVI, SAVI, IRECI, PSRI, CI_{red-edge}; b) HMSSI

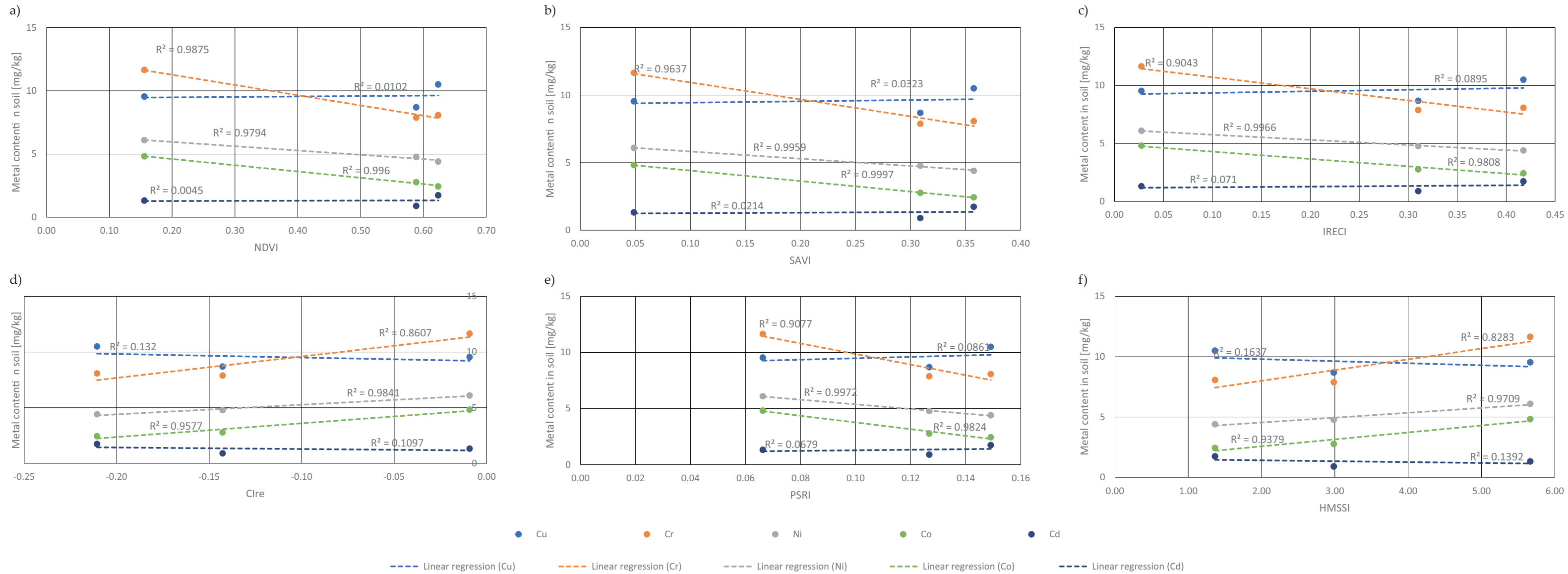


Fig. 9. Graphs of the content of selected tested heavy metals versus the values of spectral indices: a) NDVI; b) SAVI; c) IRECI; d) PSRI; e) $CI_{red-edge}$; f) HMSSI

Because of the different domain of the HMSSI spectral index compared to other indices analyzed in this paper, its results are shown in a separate chart. Standard deviations are marked with a vertical line.

The values of spectral indices for test sites A and D show a similar tendency and similar values. Figure 8a shows significantly lower values of individual indices for test site C. According to Figure 8b, the HMSSI spectral index indicates an increased pressure of heavy metals for area C compared to other areas analyzed in this study. However, a high standard deviation for HMSSI values reduces confidence in the obtained observations.

In order to check the relationship between the content of heavy metals in the soil and the values of individual spectral indices, it was decided to visualize the collected results on a dot plot (Fig. 9 on the interleaf). Because of a wide range of results, the data are grouped according to high (Pb, Zn) and low (Cu, Cr, Ni, Co, Cd) contents of heavy metals. During the qualitative analyzes, the points on the graph were searched for in such a way that it would be possible to distinguish areas with an increased content of a given heavy metal in relation to other measurement points and experimental areas. Among the seven analyzed heavy metals, a clear relationship was observed between nickel (Ni), cobalt (Co), chromium (Cr) and zinc (Zn), and the values of all spectral indices included in this study. A small number of experimental sites (only three research areas for which spectral indices were averaged) presented in the pilot study is a compelling argument for the continuation of research in order to confirm the observations.

Some observations may indicate a linear relationship to the calculated spectral indices. However, this requires the confirmation of a larger amount of test data. Table 3 presents the highest determination coefficients R^2 for heavy metals, for which a linear relationship was observed with the values of spectral indices.

Table 3. Comparison of selected heavy metals and spectral indices with the obtained determination indices R^2 in the analyzed experiment

Heavy metal	Spectral index	R^2
Ni	NDVI	0.98
	SAVI	0.99
	IRECI	0.99
	Cire	0.98
	PSRI	0.99
	HMSSI	0.97

Table 3. cont.

Heavy metal	Spectral index	R ²
Co	NDVI	0.99
	SAVI	0.99
	IRECI	0.98
	Cire	0.96
	PSRI	0.98
	HMSSI	0.94
Cr	NDVI	0.96
	SAVI	0.96
	IRECI	0.90
	Cire	0.86
	PSRI	0.91
	HMSSI	0.83
Zn	NDVI	0.89
	SAVI	0.84
	IRECI	0.74
	Cire	0.68
	PSRI	0.75
	HMSSI	0.64

6. Discussion

The understanding of the spatial and temporal dynamics of farmland processes is essential to ensure proper crop monitoring and early decision making to support efficient resource management in agriculture. Only reliable spatial information provided with a certain repeatability allows the comprehension of the influence of various factors on the environment [19]. Remote sensing techniques enable the

prediction of soil properties with a high degree of accuracy in the area of physical (texture), chemical (pH with an accuracy of more than 90%) and biological properties (organic carbon over 85%). It should be emphasized that the mentioned parameters belong to the groups of soil parameters directly related to the management of crops and optimization of agricultural production and the use of remote sensing methods allows to improve the speed of decisions made in precision agriculture at various levels of the economy [20, 22, 47].

The stage of radiometric correction of the satellite scene, including atmospheric correction is an important one in the processing of remote sensing data. Properly carried out, it allows us to significantly improve the spectral curves, as can be seen in Figures 6a and 6b. This directly translates into the values of calculated spectral indices. The limitations of remote sensing technologies for satellite imaging, resulting from long revision times or the cloud cover can be eliminated by using commercial satellite constellations (e.g., PlanetScope with 1-day revisits) or by performing a flight with unmanned aerial vehicles (UAVs) equipped with a multispectral camera [21]. Thus, the potential of remote sensing in agriculture is great and some of the technology determinants are already compensated by other frequently commercial solutions. A practical example of the discussed problem is the high cloud cover over the western test site (area B shown in Figure 1), which excluded it from further studies. In the case of having an unmanned UAV with an adapted hyperspectral camera, it would be possible to supplement the missing information about the albedo from the western region.

Despite many studies on the use of satellite remote sensing to assess the content of heavy metals in the soil, there is no single, universal mathematical model allowing such observations to be linked. In the literature review, no paper was found that would focus on estimating the possibility of using spectral index maps for qualitative assessment of soil on small agricultural plots which had not been exposed to factors of industrial activity in terms of heavy metal content. This means that the methodology for the determination of the concentration of heavy metals by indirect techniques not only differs depending on the type of cultivation and land management but also for the location of the research object and its immediate surroundings. Because of the different pace of agrotechnical treatments and the profile of their activities in agricultural areas, the level of vegetation development may vary significantly. This was reflected in the spectral curves obtained, shown in Figure 6. This is also confirmed by the results obtained in the form of maps of spectral indices presented in Figure 7. Despite the fact that in each analyzed test site there was soil after main plowing at a depth of at least 0.5 m, the maps of the NDVI and SAVI indices for the three experimental sites differed from each other (Fig. 7a, b).

The change in the spectral signal and the spectral curve due to heavy metals can be explained by the reaction of metal binding on the top mineral surface. This means that the shape of the spectral curve of the tested sample may alter as a result of changes in the chemical composition, which could additionally explain the differences in

the spectral curves of the analyzed test sites in Figure 6b. Melendez-Pastor et al. [25] made similar assumptions in their study. They reported about three-dimensional properties of soils on the basis of two forms of evidence: reference patterns of spectra and geomorphological observations supplemented with the physiological state of plants and the soil itself. The range of electromagnetic radiation commonly used in agriculture is the near infrared (800–2500 nm) and so-called red edge in a spectral range of 680–750 nm. A characteristic feature of the spectral reflection recorded in the red and near infrared channel of the electromagnetic radiation spectrum is the strong absorption of red radiation by chlorophyll and a specific peak for infrared spectral reflection in plants. According to Wang et al. [5], this phenomenon is useful to examine the content of heavy metals in plants, because the change in the amount of chlorophyll and in the results of phenological observations translates directly into plant stress and a change in the spectral curve recorded for the plant under study. Such an approach has resulted in the creation of many empirical or semi-empirical models allowing the monitoring of vegetation growth and accompanying stress [6, 11].

Diversified values of spectral indices NDVI, SAVI, IRECI, $CI_{\text{red-edge}}$, PSRI and HMSSI may indicate different physicochemical parameters of the soil in the analyzed experimental areas. Despite the fact that in each area of the experiment there was soil (without crops and visible vegetation), the values of spectral indices in the area of test site C differ from the others, which can be seen in Figure 8a. On the other hand, the HMSSI values indicate that in area C there is an increased risk of heavy metal accumulation in relation to the other test sites A and D (Fig. 8b). It was decided to check this by comparing the concentrations of the analyzed heavy metals against individual spectral indices, as shown in Figure 9. Thus, a model was sought that would help to monitor qualitatively the areas in terms of the content of heavy metals in the soil. Based on the dot plots in Figure 9 a clear relationship was observed for all the spectral indices analyzed in the study with the content of zinc (Zn), chromium (Cr), nickel (Ni), and cobalt (Co). Figures 9a and 9e allow to group areas A and D as test sites with a lower chromium content relative to the C test site, where the chromium content from in situ measurements was the highest (Tab. 2, Fig. 3).

For the measurement points created in the graphs of Figure 9, the functions were fitted with a linear regression method. Based on the obtained results, the determination index R^2 was calculated. The best match of the data was obtained for heavy metals nickel and cobalt, as shown in Table 3. Slightly lower R^2 values were obtained for zinc and chromium, where there is still a linear relationship $R^2 > 0.80$. Because of the small number of observations, the creation of advanced mathematical models allowing for remote monitoring of heavy metals in the nearby areas of the Barania Góra reserve was abandoned. This will be the subject of further research.

The main issue which determines the successful use of remote sensing techniques and spectral analyzes to determine the content of heavy metals in the soil is the optimal selection of the electromagnetic radiation band and the knowledge of

agrotechnical procedures carried out in the studied areas. In the world literature, there are papers that discuss the problems of forecasting the content of heavy metals in the soil based on remote sensing techniques using the reflectance factor [11, 25]. Nevertheless, there are many factors affecting the reflection coefficient values to be analyzed, including the applied agrotechnical measures, the application of fertilizers, and the surroundings of the studied area. The large number of the above-mentioned factors means that research on many levels and searching for relationships between various environmental parameters in a specific area of experimental test sites is required and this will be the subject of further experiments.

7. Summary and Conclusions

The procedure presented in the research shows a qualitative approach to carrying out tasks in the field of determining heavy metal concentrations in soil based on multispectral images from Sentinel-2, allowing us to identify areas with a potentially high risk of contamination with heavy metals. Conventional methods, usually consisting of taking single samples and analyzing the collected material in a laboratory, are laborious and time-consuming and do not provide full spatial information about the distribution of the parameter under study.

As part of the research, it was possible to achieve the goals set out in the introduction. An anomaly in the form of an increased cadmium content in the eastern test site was identified based on in situ measurements. Additionally, the use of spectral indices: NDVI, SAVI, IRECI, $CI_{red-edge}$, PSRI and HMSSI, to assess the content of heavy metals in the soil was positively assessed (Tab. 3) in particular the content of Ni, Co, Cr, Zn.

The conducted pilot project shows that the spectral indices: NDVI, SAVI, IRECI, $CI_{red-edge}$, PSRI and HMSSI calculated on the basis of images from Sentinel-2, have some potential to assess the content of nickel ($R^2 > 0.97$) and cobalt ($R^2 > 0.94$) on small agricultural plots (Fig. 9, Tab. 3). The calculation of determination indicators was based on only three points, so the Authors are cautious about the results obtained in the research. The confirmation of the obtained results compels us to continue the research on a larger number of experimental sites. High-resolution multispectral imaging from commercial remote sensing constellations or UAV platforms may bring much better results, and this will also be the subject of further experimental work.

Author Contributions

Author 1: conceptualization, methodology, software, data, writing – original draft preparation, visualization.

Author 2: writing – review and editing, supervision, methodology, validation.

Author 3: writing – review and editing, data, methodology.

Author 4: writing – review and editing, data, methodology.

References

- [1] D'Emilio M., Macchiato M., Ragosta M., Simoniello T.: *A method for the integration of satellite vegetation activities observations and magnetic susceptibility measurements for monitoring heavy metals in soil*. Journal of Hazardous Materials, vol. 241–242, 2012, pp. 118–126. <https://doi.org/10.1016/j.jhazmat.2012.09.021>.
- [2] *Communication from the Commission to the Council, the European Parliament, the European Economic and Social Committee and the Committee of the Regions. Thematic Strategy for Soil Protection*. Brussels, 22.09.2006, COM(2006)231 final.
- [3] Semikolennykh A.A.: *European thematic strategy for soil protection: a review of major documents*. Eurasian Soil Science, vol. 41, 2008, pp. 1349–1351. <https://doi.org/10.1134/S1064229308120168>.
- [4] Ahmed F., Dwivedi S., Shaalan N.M., Kumar S., Arshi N., Alshoabi A., Husain F.M.: *Development of Selenium Nanoparticle Based Agriculture Sensor for Heavy Metal Toxicity Detection*. Agriculture, vol. 10, 2020, 610. <https://doi.org/10.3390/agriculture10120610>.
- [5] Wang F., Gao J., Zha Y.: *Hyperspectral sensing of heavy metals in soil and vegetation: Feasibility and challenges*. ISPRS Journal of Photogrammetry and Remote Sensing, vol. 136, 2018, pp. 73–84. <https://doi.org/10.1016/j.isprsjprs.2017.12.003>.
- [6] Liu T., Liu X., Liu M., Wu L.: *Evaluating Heavy Metal Stress Levels in Rice Based on Remote Sensing Phenology*. Sensors, vol. 18(3), 2018, 860. <https://doi.org/10.3390/s18030860>.
- [7] Zhang H., Jiang L., Tanveer M., Ma J., Zhao Z., Wang L.: *Indexes of Radicle are Sensitive and Effective for Assessing Copper and Zinc Tolerance in Germinating Seeds of Suaeda salsa*. Agriculture, vol. 10, 2020, 445. <https://doi.org/10.3390/agriculture10100445>.
- [8] Yi Z., Jia L., Chen Q.: *Crop Classification Using Multi-Temporal Sentinel-2 Data in the Shiyang River Basin of China*. Remote Sensing, vol. 12, 2020, 4052. <https://doi.org/10.3390/rs12244052>.
- [9] Li M.S., Luo Y.P., Su Z.Y.: *Heavy metal concentrations in soils and plant accumulation in a restored manganese mineland in Guangxi, South China*. Environmental Pollution, vol. 147, 2007, pp. 168–175. <https://doi.org/10.1016/j.envpol.2006.08.006>.
- [10] Liu K., Zhao D., Fang J., Zhang X., Zhang Q., Li X.: *Estimation of Heavy-Metal Contamination in Soil Using Remote Sensing Spectroscopy and a Statistical Approach*. Journal of the Indian Society of Remote Sensing, vol. 45, 2017, pp. 805–813. <https://doi.org/10.1007/s12524-016-0648-4>.
- [11] Choe E., Meer F., Ruitenbeek F., Werff H., Smeth B., Kyoung-Woong K.: *Mapping of heavy metal pollution in stream sediments using combined geochemistry, field spectroscopy, and hyperspectral remote sensing: A case study of the Rodalquilar mining area, SE Spain*. Remote Sensing of Environment, vol. 112(7), 2008, pp. 3222–3233. <https://doi.org/10.1016/j.rse.2008.03.017>.

- [12] Clevers J.G.P.W., Kooistra L., Salas E.A.L.: *Study of heavy metal contamination in river floodplains using the red-edge position in spectroscopic data*. International Journal of Remote Sensing, vol. 25(19), 2004, pp. 3883–3895. <https://doi.org/10.1080/01431160310001654473>.
- [13] Gu Y.W., Li S., Gao W., Wei H.: *Hyperspectral estimation of the cadmium content in leaves of Brassica rapa chinensis based on spectral parameters*. Acta Ecologica Sinica, vol. 35(13), 2015, pp. 4445–4453 [in Chinese with English abstract].
- [14] Khabbazan S., Vermunt P., Steele-Dunne S., Ratering-Arntz L., Marinetti C., van der Valk D., Iannini L. et al.: *Crop Monitoring Using Sentinel-1 Data: A Case Study from The Netherlands*. Remote Sensing, vol. 11(16), 1887, 2019. <https://doi.org/10.3390/rs11161887>.
- [15] Hejmanowska B., Kramarczyk P., Głowienka E., Mikrut S.: *Reliable Crops Classification Using Limited Number of Sentinel-2 and Sentinel-1 Images*. Remote Sensing, vol. 13(16), 2021, 3176. <https://doi.org/10.3390/rs13163176>.
- [16] Khaliq A., Comba L., Biglia A., Ricauda Aimonino D., Chiaberge M., Gay P.: *Comparison of Satellite and UAV-Based Multispectral Imagery for Vineyard Variability Assessment*. Remote Sensing, vol. 11(4), 2019, 436. <https://doi.org/10.3390/rs11040436>.
- [17] Dad F.P., Khan W.D., Tanveer M., Ramzani P.M.A., Shaukat R., Mukhtadir A.: *Influence of Iron-Enriched Biochar on Cd Sorption, Its Ionic Concentration and Redox Regulation of Radish under Cadmium Toxicity*. Agriculture, vol. 11(1), 2021, 1. <https://doi.org/10.3390/agriculture11010001>.
- [18] Crema A., Boschetti M., Nutini F., Cillis D., Casa R.: *Influence of Soil Properties on Maize and Wheat Nitrogen Status Assessment from Sentinel-2 Data*. Remote Sensing, vol. 12(14), 2020, 2175. <https://doi.org/10.3390/rs12142175>.
- [19] Hao P., Löw F., Biradar C.: *Annual Cropland Mapping Using Reference Landsat Time Series – A Case Study in Central Asia*. Remote Sensing, vol. 10(12), 2018, 2057. <https://doi.org/10.3390/rs10122057>.
- [20] Yuzugullu O., Lorenz F., Fröhlich P., Liebisch F.: *Understanding Fields by Remote Sensing: Soil Zoning and Property Mapping*. Remote Sensing, vol. 12(7), 2020, 1116. <https://doi.org/10.3390/rs12071116>.
- [21] Messina G., Peña J.M., Vizzari M., Modica G.: *A Comparison of UAV and Satellites Multispectral Imagery in Monitoring Onion Crop. An Application in the ‘Cipolla Rossa di Tropea’ (Italy)*. Remote Sensing, vol. 12(20), 2020, 3424. <https://doi.org/10.3390/rs12203424>.
- [22] Dvorakova K., Shi P., Limbourg Q., Van Wesemael B.: *Soil Organic Carbon Mapping from Remote Sensing: The Effect of Crop Residues*. Remote Sensing, vol. 12(12), 2020, 1913. <https://doi.org/10.3390/rs12121913>.
- [23] Haneklaus S.H., Bloem E., Schnug E.: *Hungry Plants – A Short Treatise on How to Feed Crops under Stress*. Agriculture, vol. 8(3), 2018, 43. <https://doi.org/10.3390/agriculture8030043>.

- [24] Shivers S.W., Roberts D.A., McFadden J.P., Tague C.: *Using Imaging Spectrometry to Study Changes in Crop Area in California's Central Valley during Drought*. Remote Sensing, vol. 10(10), 2018, 1556. <https://doi.org/10.3390/rs10101556>.
- [25] Melendez-Pastor I., Navarro-Pedreño J., Gómez I., Almendro-Candel M.B.: *The use of remote sensing to locate heavy metal as source of pollution*. [in:] Daniels J.A. (ed.), *Advances in Environmental Research. Volume 7*, Nova Science Publishers, Hauppauge, New York 2011, pp. 225–233.
- [26] Zhang Z., Liu M., Liu X., Zhou G.: *A New Vegetation Index Based on Multi-temporal Sentinel-2 Images for Discriminating Heavy Metal Stress Levels in Rice*. Sensors, vol. 18(7), 2018, 2172. <https://doi.org/10.3390/s18072172>.
- [27] El Hajj M., Baghdadi N., Zribi M., Bazzi H.: *Synergic Use of Sentinel-1 and Sentinel-2 Images for Operational Soil Moisture Mapping at High Spatial Resolution over Agricultural Areas*. Remote Sensing, vol. 9(12), 2017, 1292. <https://doi.org/10.3390/rs9121292>.
- [28] Kavats O., Khramov, D., Sergieieva, K., Vasyliiev V.: *Monitoring Harvesting by Time Series of Sentinel-1 SAR Data*. Remote Sensing, vol. 11(21), 2019, 2496. <https://doi.org/10.3390/rs11212496>.
- [29] Dworak T., Hejmanowska B., Pyka K.: *Problemy teledetekcyjnego monitoringu środowiska. Tom 2. Teledetekcja wód i powierzchni Ziemi*. Wydawnictwa AGH, Kraków 2011.
- [30] Osińska-Skotak K.: *Metodyka wykorzystania super- i hiperspektralnych danych satelitarnych w analizie jakości wód śródlądowych*. Prace Naukowe Politechniki Warszawskiej. Geodezja, z. 47, 2010, pp. 3–153.
- [31] *Instrukcja pobierania próbek glebowych z gruntów ornych i użytków zielonych opracowana na podstawie PN-R-04031:1997*. <https://www.schr.gov.pl/index.php?c=getfile&id=31> [access: 25.09.2022].
- [32] ISO 14887:2000: *Sample Preparation – Dispersing procedures for powders in liquids*.
- [33] *Mastersizer 3000. Laser diffraction particle size analyzer*. <https://www.malvernpanalytical.com/en/products/product-range/mastersizer-range> [access: 28.10.2020].
- [34] EN 13346:2000: *Characterization of sludges – Determination of trace elements and phosphorous – Aqua regia extraction methods*. Comité européen de normalisation, Bruxelles
- [35] PN-ISO 10390:1997: *Jakość gleby – Oznaczenie pH*. Polski Komitet Normalizacyjny, Warszawa.
- [36] Kabala C., Karczewska A.: *Metodyka analiz laboratoryjnych gleb i roślin*. Wyd. 8a. Uniwersytet Przyrodniczy we Wrocławiu, Wrocław 2019. <http://karnet.up.wroc.pl/~kabala/Analizy2017v8.pdf> [access: 25.09.2022].
- [37] *Sentinel-2 Products Specification Document*. Thales Alenia Space, 2017. <https://sentinel.esa.int/documents/247904/685211/sentinel-2-products-specification-document> [access: 20.04.2022].

- [38] Louis J., Debaecker V., Pflug B., Main-Knorn M., Bieniarz J., Mueller-Wilm U., Cadau E., Gascon F.: *Sentinel-2 Sen2cor: L2A Processor for Users*. [in:] Ouwehand L. (ed.), *Proceedings of Living Planet Symposium 2016, 9–13 May 2016, Prague, Czech Republic*, SP-740, European Space Agency, 2016, pp. 1–8.
- [39] Polykretis C., Grillakis M.G., Alexakis D.D.: *Exploring the Impact of Various Spectral Indices on Land Cover Change Detection Using Change Vector Analysis: A Case Study of Crete Island, Greece*. *Remote Sensing*, vol. 12(2), 2020, 319. <https://doi.org/10.3390/rs12020319>.
- [40] Jełowicki Ł., Sosnowicz K., Ostrowski W., Osińska-Skotak K., Bakula K.: *Evaluation of Rapeseed Winter Crop Damage Using UAV-Based Multispectral Imagery*. *Remote Sensing*, vol. 12(16), 2020, 2618. <https://doi.org/10.3390/rs12162618>.
- [41] Fabre S., Gimenez R., Elger A., Rivière T.: *Unsupervised Monitoring Vegetation after the Closure of an Ore Processing Site with Multi-Temporal Optical Remote Sensing*. *Sensors*, vol. 20(17), 2020, 4800. <https://doi.org/10.3390/s20174800>.
- [42] *Rozporządzenie Ministra Środowiska z dnia 5 września 2016 r. w sprawie sposobu prowadzenia oceny zanieczyszczenia powierzchni ziemi [Ordinance of the Minister of the Environment of 5 September 2016 on how to conduct an assessment of land surface pollution]*. Dz.U. 2002 nr 165, poz. 1359.
- [43] Wang P., Chen H., Kopittke P.M., Zhao F.: *Cadmium contamination in agricultural soils of China and the impact on food safety*. *Environmental Pollution*, vol. 249, 2019, pp. 1038–1048. <https://doi.org/10.1016/j.envpol.2019.03.063>.
- [44] Krasowicz S., Oleszek W., Horabik J., Dębicki R., Jankowiak J., Stuczyński T., Jadczyński J.: *Racjonalne gospodarowanie środowiskiem glebowym Polski*. *Polish Journal of Agronomy*, vol. 7, 2011, pp. 43–58.
- [45] McCauley A., Jones C., Olson-Rutz K.: *Soil pH and Organic Matter*. *Nutrient Management Module*, no. 8, 2009, 4449-8.
- [46] Osińska-Skotak K.: *Wpływ korekcji atmosferycznej zdjęć satelitarnych na wyniki cyfrowej klasyfikacji wielospektralnej*. *Acta Scientiarum Polonorum. Geodesia et Descriptio Terrarum*, vol. 4(1), 2005, pp. 41–53.
- [47] Zagajewski B., Lechnio J., Sobczak M.: *Wykorzystanie teledetekcji hiperspektralnej w analizie roślinności zanieczyszczonej metalami ciężkimi*. *Teledetekcja Środowiska*, vol. 37, 2007, pp. 82–100.